Fabrication and Characterization of Silk Fibroin/Poly(ethylene glycol)/Cellulose Nanowhisker Composite Films

Rongji Li,[1] Yanhong Zhang,[2] Liangjun Zhu,[2] Juming Yao[1]

[1]*The Key Laboratory of Advanced Textile Materials and Manufacturing Technology of Ministry of Education, College of Materials and Textile, Zhejiang Sci-Tech University, Hangzhou 310018, China*
[2]*Institute of Applied Bioresource, College of Animal Sciences, Zhejiang University, Hangzhou 310029, China*

Received 18 May 2010; accepted 16 July 2011
DOI 10.1002/app.35273
Published online 25 October 2011 in Wiley Online Library (wileyonlinelibrary.com).

ABSTRACT: The flexible and transparent composite films were fabricated by a mixture of silk fibroin (SF), poly(ethylene glycol), and mulberry cellulose nanowhiskers (CNWs). The CNWs were uniformly dispersed in the matrix when its content was as high as 12 w/w%. The tensile properties of composite films generally depended on the nanowhisker content, but significantly improved when compared to the pure SF film. DMA analysis revealed that the alpha transition temperature increased gradually with the increase of nanowhisker content, probably due to the formation of interactions between the nanowhiskers and the SF molecular chains, leading to the mobility reduction of the amorphous SF.
 J Appl Polym Sci 124: 2080–2086, 2012

Key words: nanocomposites; films; reinforcement; silk fibroin; cellulose nanowhisker

INTRODUCTION

Silk fibroin (SF) is a fibrous protein isolated from the cocoon fiber of *Bombyx mori* (*B. mori*) silkworm. Besides being as the textile material, SF fibers in the form of suture have been used for centuries.[1] In the past decades, the regenerated SF solution was used to prepare the biomaterials with various geometries including films,[2] 3D scaffolds,[3] hydrogels,[4] and nonwoven mats[5] for enzyme-immobilization, contact lens, wound dressing, and bone/cartilage tissue engineering, etc. Among these, *B. mori* SF films were primarily used as the substrates for the enzyme immobilization in biosensors.[2,6,7] The glucose sensor was prepared with a glucose oxidase (GOD)-immobilized SF film attached on an oxygen electrode surface and assembled in the apparatus[6]; biophotosensors could be made using fibroin films with immobilized peroxidase.[7] With the development of tissue engineering, the application of SF films was broadened in the biomedical field sometimes by surface modification or by blending with other polymers.[1,8] For example, the recent researches on the SF films showed its potential application to be explored as the cornea tissue replacement materials.[9,10] The as-prepared SF films from the regenerated SF solution usually have silk I crystalline structure, leading to the brittleness and poor flexibility. Some treatments of SF film, e.g., soaking in ethanol solution, can improve the mechanical properties and reduce the degradability due to the structural transition of SF from silk I to silk II. However, such a structural transition leads to the reduction of water vapor and oxygen permeability, and the alcohol treatment usually causes a significant shrinkage of films.[11] It was reported that the mechanical properties of SF film could be enhanced by blending SF with other polymers like poly(vinyl alcohol) [12] and cellulose.[13] Recently, the cellulose nanowhiskers (CNWs) have attracted a lot of attention in the material reinforcement for its natural and renewable origins as well as the impressive mechanical properties.[14–17] The CNWs can be prepared by a controlled acid hydrolysis of different sources like cotton,[15] tunicate,[14] and sisal.[17] Noishiki et al.[18] prepared the SF-microcrystalline cellulose (cellulose whisker from tunicate) composite films with varied compositions. The tensile strength and ultimate strain of the composite films showed a maximum at 70–80% cellulose content, reaching five times those of fibroin-alone or cellulose-alone films, but the ultimate strain was actually quite low at about 4%. Poly(ethylene glycol) (PEG), a biodegradable water-soluble polymer, is one of the widely used plasticizers, lowering the glass-rubber transition

Correspondence to: J. Yao (yaoj@zstu.edu.cn).
Contract grant sponsor: Program for Changjiang Scholars and Innovative Research Team in University; contract grant number: IRT0654.
Contract grant sponsor: Program for New Century Excellent Talents in University; contract grant number: NCET070763.

temperature (T_g) of matrix and making it much extensible.[19] However, the use of plasticizer unavoidably leads to a significant decrease of tensile strength. In this work, the effect of CNW content on the reinforcement of SF films was investigated. To improve the flexibility of composite films, PEG was used as the plasticizer at the content of 30 w/w%. The flexible SF/PEG/CNW composite films were macroscopically homogeneous and transparent, which were then characterized by FE-SEM, AFM, XRD, DMA, and mechanical testing.

EXPERIMENTAL

Preparation of SF solution

B. mori silkworm cocoons, obtained from Huzhou Acadamy of Agricultural Sciences (Huzhou, China), were degummed three times with 0.5 w/v % Marseilles soap solution at 100°C for 30 min and washed with distilled water to remove the glue-like sericin protein. The degummed SF fibers were then dissolved in a $CaCl_2$ aqueous/ethanol solution (molar ratio, $CaCl_2/C_2H_5OH/H_2O = 1/2/8$) at 70–75°C for 2 h, followed by a dialysis against distilled water for 3 days. The final concentration of SF in the solution was 3 w/w%, which was determined by the bradford protein assay on a DNA/Protein Analyzer (DU530, Beckman Coulter Inc., USA).

Preparation of mulberry CNWs

Morus alba L. mulberry branch barks were also obtained from Huzhou Acadamy of Agricultural Sciences (Huzhou, China). The preparation of mulberry CNWs has been described previously.[20] Briefly, the mulberry bark pieces were pretreated with 1 w/v% NaOH solution at 80°C for 2 h followed by washing with adequate water. A high temperature degumming process was carried out in a chamber (ES-315, Tomy Seiko, Japan) by soaking the pretreated barks into a solution containing 1 w/v% NaOH and 1 w/v% Na_2S with a bath ratio of 1 : 30 at 130°C for 1.5 h to obtain the mulberry fibers. The mulberry fibers were washed with distilled water, followed by hydrolysis with 64 w/w% sulfuric acid at 60°C for 30 min under vigorous stirring to obtain the CNW suspension. The suspension was diluted by cold water and washed to neutrality by successive centrifugation at 10,000 rpm at 10°C for 10 min, and dialyzed against distilled water. The suspension was stored in a refrigerator at 4°C with some drops of chloroform to avoid the bacterial growth.

Fabrication of composite films

Three components, SF solution, PEG 400, and mulberry CNW suspension, were mixed together under stirring gently (~ 100 rpm to avoid the SF aggregation) for 2 h, which were cast onto the polystyrene disks and dried in an incubator at 25°C to obtain the composite films. Here, the PEG content in the composite films was fixed at 30 w/w%, and the CNW content was varied from 0 w/w% to 15 w/w% with an interval of 3 w/w%. The obtained composite films were named as SF/PEG/CNW-0, SF/PEG/CNW-3, SF/PEG/CNW-6, SF/PEG/CNW-9, SF/PEG/CNW-12, and SF/PEG/CNW-15 corresponding to the CNW content varied from 0 to 15 w/w%. The pure SF film was prepared for comparison.

Characterizations

A drop of diluted CNW suspension was deposited on the carbon-coated copper grid. Transmission electron microscopy (TEM) was observed on a microscope (JEM-1230, JEOL, Japan) operated at an acceleration voltage of 120 kV. For the field emission scanning electron microscopy (FE-SEM) observation, the composite films were cooled in the liquid nitrogen for 5 s, and then fractured and coated with gold. The morphology of fracture surfaces was examined on a microscope (*S*-4800, Hitachi, Japan) with an accelerating voltage of 5 kV. The surface morphology of composite films was characterized on an atomic force microscopy (AFM) (XE-100E, PSIA, Korea) using noncontact mode. The roughness of surface was analyzed by XEI imaging software (ver. 1.6.1 Alpha, PSIA, Korea).

The X-ray diffraction (XRD) patterns of the composite films were obtained at ambient temperature by step scanning on an X-ray powder diffractometer (ARL X'TRA, Thermo Electron Corp., USA) using a monochromatic CuKα radiation ($\lambda = 1.54$ Å) in the range of $2\theta = 10°–50°$ with a step size of 0.04° and a scanning rate of 5.0° min^{-1}.

Dynamical mechanical analysis (DMA) of the composite films was carried out on a DMA equipment (Q-800, TA Instruments, USA) using the tensile mode. The temperature scanning from ambient temperature to 250°C was performed with a constant heating rate of 3°C min^{-1} at an oscillation frequency of 1 Hz and a strain amplitude of 0.05%. The rectangular profile of the samples was used (15×10 mm^2).

The mechanical properties were carried out on a mechanical testing equipment (AG-1, Shimadzu, Japan) with a 50N load cell at a crosshead speed of 10 mm min^{-1}. The tests were conducted at a temperature of 20°C and a relative humidity of 65% after an equilibration in the controlled environment for at least 24 h. The rectangular profile of the samples was used (20×10 mm^2). The data reported were the mean of 5 measurements.

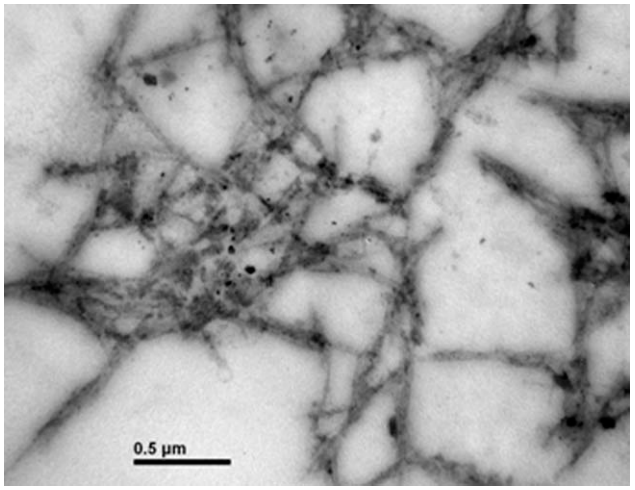

Figure 1 TEM micrograph of mulberry CNWs.

RESULTS AND DISCUSSION

Morphology of CNWs and composite films

Figure 1 shows the TEM micrograph of mulberry CNWs, where the whiskers dispersed uniformly. The diameter of whiskers was ranged from 20 to 40 nm with a length of ~ 500 nm. Figure 2 shows the FE-SEM images of the fracture surface of different films, where the inserts are the photographs of each film. The photographs showed that the films had similar transparency at different compositions. When compared to pure SF film [Fig. 2(a)], the fracture surface of SF/PEG/CNW-0 [Fig. 2(b)] remained its smooth character, where only a few cracks could be found suggesting that SF and PEG were well mixed. At a low CNW content level of 3 w/w% [Fig. 2(c)], the CNWs were hard to be found. However, as the content was up to 6 w/w% [Fig. 2(d)], the CNWs were easily identified as the white dots,[21] which was gradually increased with the increase of CNW content in the composite films. A uniform distribution of CNWs in the matrix could be seen from all the composites, which is essential to obtain optimum mechanical properties. Further comparison of the FE-SEM images of SF/PEG/CNW-12 and SF/PEG/CNW-15 at higher magnification was shown in Figure 2(h,i), where the difference of CNW distribution was observed. The CNWs in SF/PEG/CNW-12 mostly appeared as tiny white dots consistent with the diameter of individual CNWs. However, the whiskers aggregated together showing larger dots in

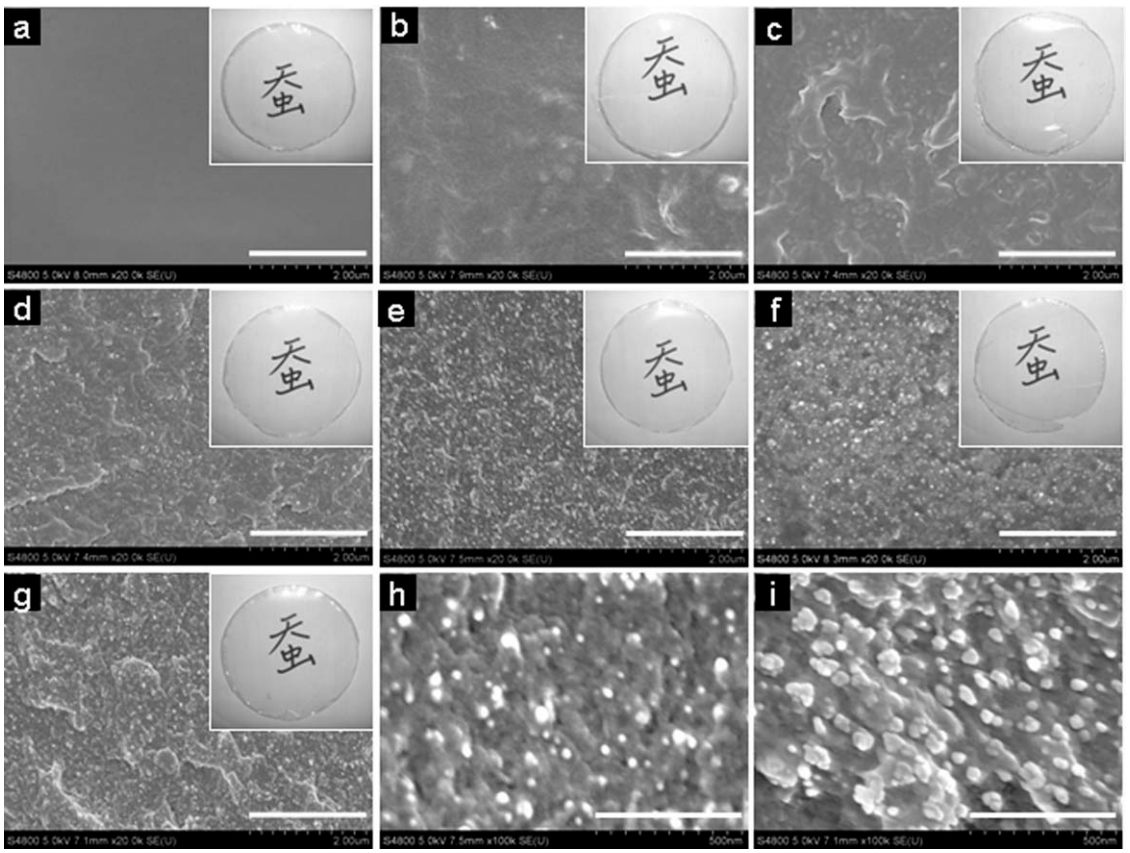

Figure 2 FE-SEM images of the fracture surface of (a) pure SF film, (b) SF/PEG/CNW-0, (c) SF/PEG/CNW-3, (d) SF/PEG/CNW-6, (e) SF/PEG/CNW-9, (f) SF/PEG/CNW-12, and (g) SF/PEG/CNW-15. (h) and (i) were the images of SF/PEG/CNW-12 and SF/PEG/CNW-15, respectively, at higher magnification. The inserts were the photographs showing the appearance of different films. Scale bars, (a)–(g) 2 μm; (h) and (i) 500 nm.

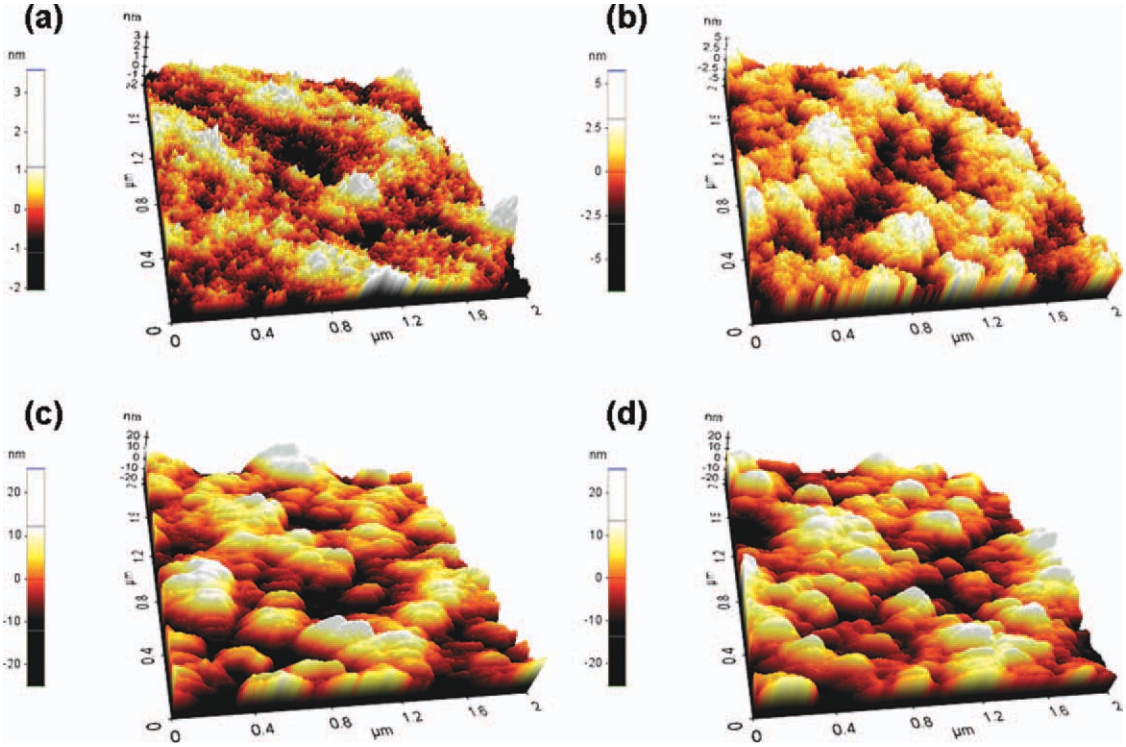

Figure 3 AFM images of (a) pure SF film, (b) SF/PEG/CNW-0, (c) SF/PEG/CNW-6, and (d) SF/PEG/CNW-12. Each image was 2 μm by 2 μm. [Color figure can be viewed in the online issue, which is available at wileyonlinelibrary.com].

the SF/PEG/CNW-15, which may be due to the excessive filling of CNWs.

Figure 3 shows the AFM images of selected four films, i.e., pure SF film, SF/PEG/CNW-0, SF/PEG/CNW-6, and SF/PEG/CNW-12. Generally, the pure SF film was extremely smooth with no evidence of surface irregularity observed, which has a root-mean-square (RMS) roughness of 0.56 nm. A slight increase of surface roughness was observed on the SF/PEG/CNW-0, which had a RMS roughness of 1.49 nm. However, after adding the CNWs into the composite films, the surface morphology changed remarkably. The RMS roughness was increased to 6.15 nm for SF/PEG/CNW-6 and 6.92 nm for SF/PEG/CNW-12, respectively.

Structure of composite films

Figure 4 shows the XRD patterns of composite films, where the patterns of pure SF film and CNWs were also shown for comparison. The XRD pattern of pure SF film [Fig. 3(a)] exhibited a broad hump at $2\theta = 23.9^\circ$, indicating an amorphous structure of the film. However, the diffraction pattern of SF/PEG/CNW-0 shows a distinct peak at $2\theta = 20.6^\circ$, suggesting a structural transition occurred in SF and the improvement of crystallization attributed to the interaction between the PEG molecules and SF peptide chains. With the addition of CNWs in the PEG plasticized composite films, the diffraction peaks became sharp at $2\theta = 22.8^\circ$ and other two broad peaks at $2\theta = 15.3^\circ$ and 16.7° were observed, which were ascribed to the CNWs. No evidence of any additional peaks or peak shift was observed, indicating that the diffraction patterns of composite films were only the superimposition of the two components.

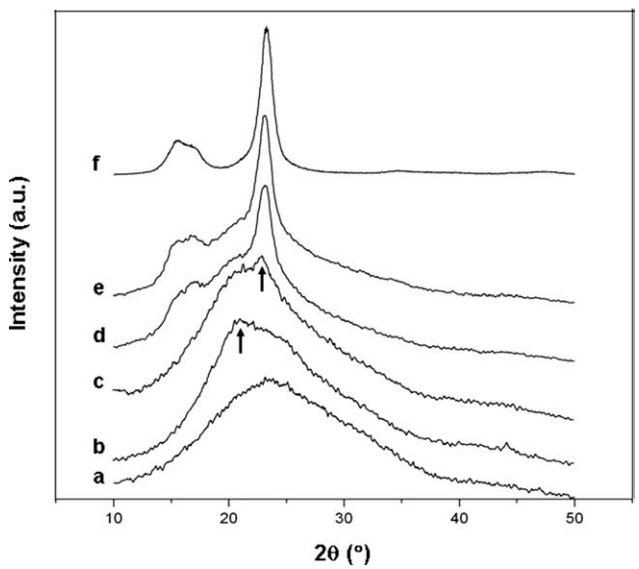

Figure 4 XRD patterns of (a) pure SF film, (b) SF/PEG/CNW-0, (c) SF/PEG/CNW-3, (d) SF/PEG/CNW-9, (e) SF/PEG/CNW-15, and (f) CNWs.

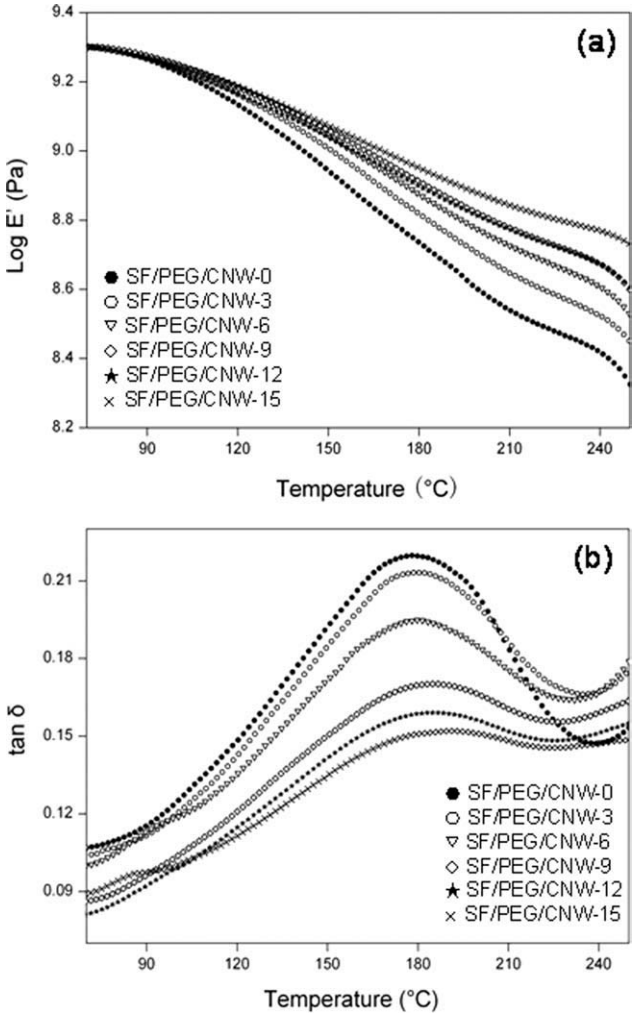

Figure 5 Evolution of (a) storage modulus and (b) tan δ as a function of temperature from DMA analysis of different composite films.

Dynamic mechanical analysis

Figure 5(a) shows the logarithm evolution of the storage tensile modulus at 1 Hz as a function of temperature for the composite films. It is well-known that the exact determination of the glassy modulus depends on the precise knowledge of the sample dimensions. In this case, to minimize this effect, the storage tensile modulus, E', at 70°C was normalized at 2.0 GPa for all the samples, which was an average value of five replicates. This can be justified by the fact that the difference between the elastic moduli of the glassy polymer and mulberry cellulose filler was not high enough to easily appreciate any change at the low filler loading used in this study.

In Figure 5(a), the curve of SF/PEG/CNW-0 shows the typical thermoplastic behavior. At the temperature below 120°C, the PEG-plasticized SF matrix was in the glassy state and the storage modulus decreases slightly with the increase of temperature. At the high temperature, a continuous decrease of elastic modulus was observed, corresponding to the primary relaxation associated with the glass-rubber transition of amorphous SF. This modulus decrease due to the energy dissipation displayed the concomitant relaxation in Figure 5(b) where tan δ passed through a maximum. The large span of this process implied a considerable broadening of the glass transition. The decline trend of modulus slowed down and reached a "plateau" at around 210°C, corresponding to the rubbery state in which the amorphous chains entangled together.

CNWs have the reinforcing effect on the composite modulus as shown in Figure 5(a) especially at temperature higher than T_g. Compared to the SF/PEG/CNW-0, the modulus was substantially increased with the increase of CNWs in the composite films, which may be ascribed to the formation of a rigid whiskers' network governed by a percolation mechanism within the host matrix.[22] Table I listed the alpha transition temperature (T_α) during the relaxation process associated with the anelastic manifestation of the glass-rubber transition of the amorphous domains in the composite films. Here, a shift of T_α toward high temperature was observed with the increase of CNW content, suggesting a reduced mobility of amorphous SF chains in the presence of interactions between the CNWs and the matrix. On the other hand, the altitude of tan δ peak at T_α (I_α) decreased with the increase of CNW content as shown in Figure 5(b) and Table I, which may be ascribed to the decrease of mobile units of SF participating in the relaxation process.

Tensile testing

Figure 6 shows the typical tensile stress–strain curves of different composite films. The pure SF film shows a brittle fracture at low strain of ~ 2%, whereas the PEG-plasticized SF (SF/PEG/CNW-0) has a thermoplastic tensile behavior. The SF/PEG/CNW-0 could undergo a large deformation before breaking, which had the stain at break of nearly 100% with dropping on the tensile strength by half to ~ 20 MPa when compared to the pure SF film. On the other hand, the reinforcing of CNWs on the

TABLE I
Alpha Transition Temperature (T_α) and Its Altitude (I_α) During the Relaxation Process of the Amorphous Domains in the Composite Films

Samples	T_α (°C)	I_α
SF/PEG/CNW-0	178.4	0.220
SF/PEG/CNW-3	180.1	0.204
SF/PEG/CNW-6	180.0	0.187
SF/PEG/CNW-9	185.4	0.164
SF/PEG/CNW-12	186.1	0.153
SF/PEG/CNW-15	190.8	0.147

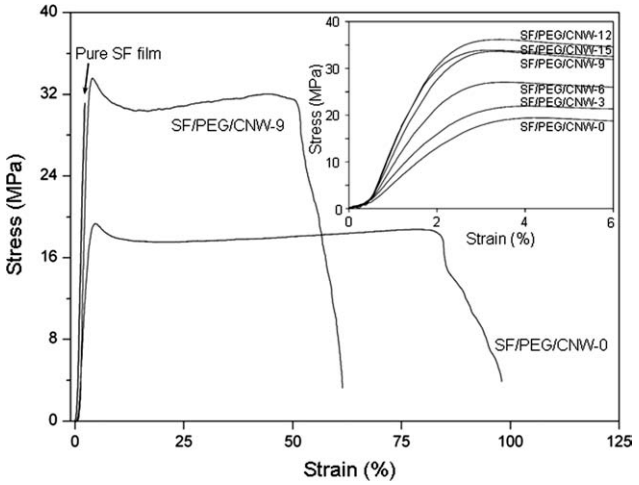

Figure 6 Typical tensile stress–strain curves of different composite films. Insert was the typical curves of different composite films at low strain.

tensile strength of composite films was clear. The tensile strength of SF/PEG/CNW-9 reached to 33 MPa, which is similar to the pure SF film. Meanwhile, the strain at break of SF/PEG/CNW-9 reduced to ~ 55%, displaying a ductile behavior with enhanced mechanical strength simultaneously. The insert in Figure 6 shows the typical tensile stress–strain curves of six composite films at low strain. The evolution of Young's modulus determined from the initial slope of stress–strain curves was plotted in Figure 7(a). The SF/PEG/CNW-0 had the Young's modulus of ~ 800 MPa, which was less than half of that of pure SF film (data not shown). This reduction of modulus was absolutely resulted from the plasticization of PEG. The incorporation of plasticizers primarily aims at reducing the brittleness of the polymeric films. Here, the PEG chains may form a ductile PEG-rich phase separated from the SF domains, which acted as the second phase dispersed in the SF continuous phase and furthermore relieved the interaction between SF peptide chains.[23]

A remarkable increasing tendency of the Young's modulus of the composite films was observed with the increase of CNW content. The Young's modulus of SF/PEG/CNW-9 was more than 2.5 times higher than that of SF/PEG/CNW-0. Noishiki et al.[18] reported that there was a conformational change of SF chains from a random coil to an ordered structure related to the highly ordered surface of cellulose whiskers. They found that in the tunicin whiskers reinforced SF films, the cellulose surface caused morphological modifications of SF chains and the highly ordered tunicin whiskers surface induced the silk crystallization at the filler-matrix interface. Nevertheless, in this work, when the CNW content reached as high as 15 w/w%, the Young's modulus of SF/PEG/CNW-15 slightly decreased when compared to that of SF/PEG/CNW-12. This is probably due to the aggregation of CNWs in the SF matrix as observed from the FE-SEM micrographs.

Figure 7(b) shows the evolution of tensile strength and strain at break for the composite films with the increase of CNW content. Similar to the evolution of the Young's modulus, the tensile strength of the composite films increased significantly from 20 to 36 MPa with the increase of CNW content from 0 to 12 w/w%, followed with a decrease to 33 MPa when the CNW content was 15 w/w%. Meanwhile, the strain at break decreased from 92 to 10%, bust still significantly larger than that of SF/CNW composite films reported by Noishiki et al.[18] Indeed, not only the filler-matrix adhesion but also the filler-filler interactions are important when considering the reinforcing capability of cellulose whiskers. The composite films obtained by a casting/evaporation process have high mechanical performance compared to freeze-drying/molding and freeze-drying/extruding/molding techniques. This discrepancy was suggested to be due to the predominance of the whisker/whisker interactions and their contribution

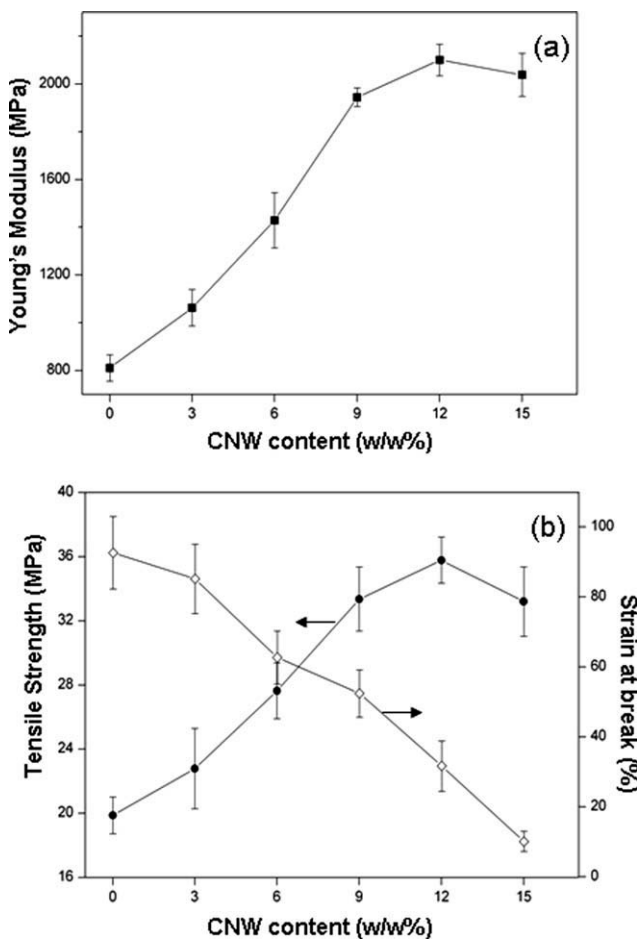

Figure 7 (a) Young's modulus, (b) tensile strength and strain at break for the composite films prepared with different CNW contents.

to the overall reinforcing effect in the evaporated films in relation to homogeneous fillers dispersion into the matrix and the sedimentation phenomenon.[24]

CONCLUSIONS

The CNWs extracted from the mulberry barks were used to reinforce the PEG-plasticized SF film, in which a uniform dispersion of CNWs in the SF/PEG matrix could be achieved when the CNW content was as high as 12 w/w%. Further increase of CNW content led to the aggregation of nanowhiskers. The flexible and transparent composite films were obtained, whose tensile properties obviously depended on the CNW content. DMA analysis revealed that the alpha transition temperature during relaxation process of the composite films appeared at around 180°C, which increased gradually with the addition of PEG and the increase of CNW content due to the reduction on the mobility of amorphous SF chains. This kind of flexible and transparent SF-matrix composite films may possess the potential utilizations in the extended biomedical application fields.

References

1. Vepari, C.; Kaplan, D. L. Prog Polym Sci 2007, 32, 991.
2. Zhang, Y. Q. Biotech Adv 1998, 16, 961.
3. Nazarov, R.; Jin, H. J.; Kaplan, D. L. Biomacromolecules 2004, 5, 718.
4. Motta, A.; Migliaresi, C.; Faccioni, F.; Torricelli, P.; Fini, M.; Giardino, R. J Biomater Sci Polym Ed 2004, 15, 851.
5. Li, C.; Vepari, C.; Jin, H. J.; Kim, H. J.; Kaplan, D. L. Biomaterials 2006, 27, 3115.
6. Demura, M.; Asakura, T. Biotechnol Bioeng 1989, 33, 598.
7. Wu, Y. H.; Shen, Q. C.; Hu, S. S. Anal Chim Acta 2006, 558, 179.
8. Wang, Y.; Kim, H. J.; Vunjak-Novakovic, G.; Kaplan, D. L. Biomaterials 2006, 27, 6064.
9. Chirila, T.; Barnard, Z.; Zainuddin; Harkin, D. G.; Schwab, I. R.; Hirst, L. Tissue Eng Part A 2008, 14, 1203.
10. Lawrence, B. D.; Marchant, J. K.; Pindrus, M. A.; Omenetto, F. G.; Kaplan, D. L. Biomaterials 2009, 30, 1299.
11. Minoura, N.; Tsukadab, M.; Nagurac, M. Polymer 1990, 31, 265.
12. Tsukada, M.; Freddi, G.; Crighton, J. S. J Polym Sci B Polym Phys 1994, 32, 243.
13. Freddi, G.; Romanò, M.; Massafra, M. R.; Tsukada, M. J Appl Polym Sci 1995, 56, 1537.
14. Capadona, J. R.; Shanmuganathan, K.; Tyler, D. J.; Rowan, S. J.; Weder, C. Science 2008, 319, 1370.
15. Paralikara, S. A.; Simonsenb, J.; Lombardic, J. J Membr Sci 2008, 320, 248.
16. Petersson, L.; kvien, I.; Oksman, K. Comp Sci Tech 2007, 67, 2535.
17. Siqueira, G.; Bras, J.; Dufresne, A. Biomacromolecules 2009, 10, 425.
18. Noishiki, Y.; Nishiyama, Y.; Wada, M.; Kuga, S.; Magoshi, J. J Appl Polym Sci 2002, 86, 3425.
19. Paul, M. A.; Alexandre, M.; Degee, P.; Henrist, C.; Rulmont, A.; Dubois, P. Polymer 2003, 44, 443.
20. Li, R. J.; Fei, J. M.; Cai, Y. R.; Li, Y. F.; Feng, J. Q.; Yao, J. M. Carbohydr Polym 2009, 76, 94.
21. Cao, X.; Dong, H.; Li, C. M. Biomacromolecules 2007, 8, 899.
22. Dufresne, A.; Witholt, B.; Kellerhals, M. B. Macromolecules 1999, 32, 7396.
23. Bayraktar, O.; Malay, Ö.; Özgarip, Y; Batıgün, A. Eur J Pharm Biopharm 2005, 60, 373.
24. Dufresne, A.; Cavaillé, J. Y.; Helbert, W. Polym Compos 1997, 18, 198.